

## Topological Flat Bands in Graphene Super-Moiré Lattices

Mohammed M. Al Ezzi<sup>1,2</sup>, Junxiong Hu<sup>1,2</sup>, Ariando Ariando,<sup>2</sup> Francisco Guinea,<sup>3</sup> and Shaffique Adam<sup>1,2,4,5</sup>


<sup>1</sup>Centre for Advanced 2D Materials, National University of Singapore, 6 Science Drive 2, Singapore 117546

<sup>2</sup>Department of Physics, Faculty of Science, National University of Singapore, 2 Science Drive 3, Singapore 117542

<sup>3</sup>IMDEA Nanociencia, C/ Faraday 9, 28049 Madrid, Spain

<sup>4</sup>Department of Materials Science and Engineering, National University of Singapore, 9 Engineering Drive 1, Singapore 117575

<sup>5</sup>Yale-NUS College, 16 College Avenue West, Singapore 138527

 (Received 3 July 2023; revised 6 December 2023; accepted 13 February 2024; published 18 March 2024)

Moiré-pattern-based potential engineering has become an important way to explore exotic physics in a variety of two-dimensional condensed matter systems. While these potentials have induced correlated phenomena in almost all commonly studied 2D materials, monolayer graphene has remained an exception. We demonstrate theoretically that a single layer of graphene, when placed between two bulk boron nitride crystal substrates with the appropriate twist angles, can support a robust topological ultraflat band emerging as the second hole band. This is one of the simplest platforms to design and exploit topological flat bands.

DOI: [10.1103/PhysRevLett.132.126401](https://doi.org/10.1103/PhysRevLett.132.126401)

**Introduction.**—Since the initial isolation of graphene, these 2D sheets of carbon atoms have shown remarkable electronic properties [1,2]. Despite early expectations to the contrary [3], the properties of monolayer graphene are mostly understood in a weakly interacting framework [4]. There have been numerous proposals to modify graphene's electronic properties [5]; the most dramatic of these is applying an external moiré periodic potential [6]. Although moiré potentials in graphene induced by a hexagonal boron nitride substrate modify several of its electronic properties—including the emergence of secondary Dirac points [7] and electronic band gaps [8–10]—the system remains weakly correlated.

Twisted bilayer graphene was the first moiré-based system to show signatures of strong electron-electron interactions, a consequence of their very flat bands [11] that are often topological [12]. Experiments in such twisted moiré graphene have observed several interesting phenomena including superconductivity [13], correlated insulators [14], ferromagnetism [15], fractional Chern insulators [16], etc. Beyond twisted bilayers, correlated physics has also been seen in many families of graphene-based materials with single-moiré potentials including twisted monolayer-bilayer [17–19], twisted double-bilayer [20], and twisted multilayer graphene systems [21].

A double moiré is defined as perturbing a 2D material with two distinct moiré potentials. This can be accomplished by encapsulating graphene with top and bottom *h*-BN substrates [22–24] or using a very recently demonstrated configuration [25] where three graphene layers are twisted relative to each other with two unconstrained angles. This often results in nonperiodic or quasiperiodic potentials. A special case of the double-moiré potential is a

super-moiré lattice potential, where the two moiré potentials are commensurate but not identical.

In this Letter, we demonstrate that a super-moiré lattice potential applied to monolayer graphene induces a flat, stable, and well-separated topological band that is likely to give correlated physics similar to other graphene-based moiré systems. Since this just involves a single carbon layer encapsulated by bulk *h*-BN crystals, our proposal is the minimal setup required to observe correlated moiré physics in a graphene-based system and could serve as the Rosetta stone for understanding correlated phenomena in other more complicated twisted configurations. We also find similar topological flat bands in encapsulated Bernal bilayer graphene and in rhombohedral graphene trilayers making our proposed scheme very generic.

Since monolayer graphene and hexagonal boron nitride (*h*-BN) are the two most prominent two-dimensional van der Waals materials and are commonly used in stacked combinations, one might ask if such a configuration has been previously studied. It is well known that single-moiré superlattices lead to significant modifications to the optical and electronic properties of monolayer graphene, but the electronic bands are not flat and do not show signs of correlation physics [8]. However, some existing double-moiré devices could have unintentionally formed a commensurate super-moiré lattice potential, for example, and our proposal might have already been observed in recent experiments where about 8% of their double-moiré samples showed signatures of flat bands and possible correlated behavior [26]. With new experimental advances [27] to control the substrate alignment, it is now possible to reliably engineer such super-moiré potentials, making it feasible to test these predictions. Although there are some

exotic proposals for generating flat bands in monolayer graphene, e.g., by applying a periodic strain profile [28], to our knowledge, inducing a topological flat band in monolayer graphene by pure moiré potentials has not previously been discussed.

*Model.*—The effect of  $h$ -BN on the electronic and optical properties of graphene in G/ $h$ -BN heterostructures is typically included either employing an effective periodic potential [29–31] or by adopting the original continuum model for twisted bilayer graphene [6,11] but replacing one graphene layer with  $h$ -BN [32]. Both these approaches have had considerable success in modeling single-moiré potentials. These models have also been used to study double-aligned-moiré potentials both with [33] and without [26] a relative displacement between the two  $h$ -BN stacks. To model a super-moiré lattice potential, we generalize these approaches using a Hamiltonian symbolically represented by the following  $3 \times 3$  matrix:

$$H = \begin{bmatrix} H_{\text{bottom-}h\text{-BN}} & B^\dagger & 0 \\ B & H_A & T^\dagger \\ 0 & T & H_{\text{top-}h\text{-BN}} \end{bmatrix}, \quad (1)$$

where  $H_A$  is the effective Hamiltonian for the “active” graphene subsystem (e.g., monolayer, Bernal bilayer, or rhombohedral trilayer graphene considered here) encapsulated by top and bottom  $h$ -BN stacks with Hamiltonians  $H_{\text{top-}h\text{-BN}} = H_{\text{bottom-}h\text{-BN}} = \text{diag}(V_N, V_B)$ , respectively. We use  $(V_N, V_B) = (-1400, 3340)$  meV for the on-site energies for nitrogen and boron atoms [32]. We have verified that incorporating the overlap between B and N atoms [34]—specifically, the off-diagonal terms in the block Hamiltonian of  $h$ -BN—has no impact on our results. Additionally, the inclusion of extra layers in the  $h$ -BN Hamiltonian makes no visible difference to our findings [35]. (Details can be found in Supplemental Material [36].)

$B$  and  $T$  represent the moiré coupling matrices that couple electronic states of the graphene subsystem with electronic states of the bottom and top  $h$ -BN stacks, respectively.

Following the usual convention (see, e.g., Refs. [31,32,37]), we fix the lattice vectors  $a_1 = a(1, 0)$  and  $a_2 = a[\frac{1}{2}, (\sqrt{3}/2)]$ , where  $a = 0.246$  nm. The lattice vectors of the rotated  $h$ -BN stacks are  $a_i^{T/B} = MR(\theta^{T/B})a_i$ , where  $R(\theta^{T/B})$  is the rotation matrix parametrized by the amount of twist angle for top  $\theta^T$  and bottom  $\theta^B$   $h$ -BN stacks and  $M = a_{h\text{-BN}} = 1.018a$ . Stacking graphene with a given  $h$ -BN substrate leads to a hexagonal single-moiré structure with lattice vectors given by  $L_i^{T/B} = [1 - R(\theta^{T/B})^{-1}M^{-1}]a_i$ . The super-moiré lattice occurs when the top and bottom moiré potentials are commensurate but not aligned. The super-moiré potential

is hexagonal and its primitive lattice vectors are given by

$$\begin{pmatrix} L_1 \\ L_2 \end{pmatrix} = \begin{pmatrix} \alpha & \beta \\ -\beta & \alpha + \beta \end{pmatrix} \begin{pmatrix} L_1^T \\ L_2^T \end{pmatrix}, \quad (2)$$

where  $\alpha$  and  $\beta$  are the super-moiré lattice integers. The two rotation angles  $\theta^{T/B}$  and the super-moiré lattice integers for the top and bottom moiré potentials are determined by satisfying the following relation:

$$\begin{pmatrix} \alpha & \beta \\ -\beta & \alpha + \beta \end{pmatrix} \begin{pmatrix} L_1^T \\ L_2^T \end{pmatrix} = \begin{pmatrix} \gamma & \delta \\ -\delta & \gamma + \delta \end{pmatrix} \begin{pmatrix} L_1^B \\ L_2^B \end{pmatrix}. \quad (3)$$

For concreteness, we align the bottom  $h$ -BN stack with the graphene active subsystem  $\theta^B = 0$  and fix the top  $h$ -BN stack twist angle to be  $\theta^T \approx 0.6^\circ$ . These are the smallest angles that generate a super-moiré potential (we discuss other examples at the end). This configuration corresponds to setting  $(\alpha = 0, \beta = 2, \gamma = 1, \delta = 1)$  in the equation above and completely specifies our model for the super-moiré periodic structure. To solve our Hamiltonian (1), we expand in the plane wave basis of the graphene subsystem and top and bottom  $h$ -BN stacks and then couple them with the  $B$  and  $T$  matrices given by

$$\{T(r), B(r)\} = w \sum_{j=0}^3 t_j \left\{ e^{-iq_j^{\text{top}} \cdot r}, e^{-iq_j^{\text{bottom}} \cdot r} \right\},$$

$$t_j = \sigma_0 + \cos\left(\frac{2\pi}{3}j\right)\sigma_x + \sin\left(\frac{2\pi}{3}j\right)\sigma_y, \quad (4)$$

where  $w = 150$  meV is the strength of the moiré potential energy and  $q_j^{T/B}$  are the moiré tunnelling vectors associated with  $L_i^{T/B}$ .

*Results.*—Figure 1 shows our main result. The left and right panels show two different configurations and their corresponding band structures. The left panel shows a double-aligned-moiré potential (studied, for example, in Refs. [26,33]). We find the band structure for this case does not feature flat bands (in agreement with previous studies). For the super-moiré lattice configuration considered here, the electronic structure shows qualitative differences. In particular, as shown in Fig. 1(d), we find a flat topological band with Chern number 1.

To further understand how this flat band emerges and examine its robustness, we apply the formalism of Ref. [29], which is a general symmetry-based approach to model the effects of  $h$ -BN on graphene electronic states. For example, using this approach, these authors were able to demonstrate that, by parametrically tuning the coupling parameters, graphene with a single-moiré potential supported mini-Dirac points at different points in the mini-Brillouin zone. Applying this approach to the super-moiré

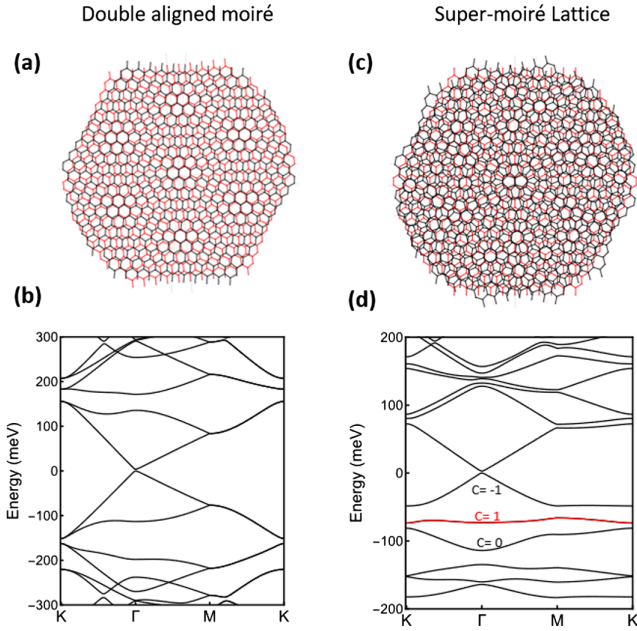


FIG. 1. Topological flat band in monolayer graphene with a super-moiré lattice potential. (a) Schematic of a double-aligned-moiré potential where the top and bottom layers have the same twist angle ( $\theta = 0.6^\circ$ ). (b) The corresponding band structure does *not* have flat bands. (c) Schematic of a super-moiré lattice potential formed when monolayer graphene is encapsulated by slightly misaligned  $h$ -BN substrates ( $\theta_B = 0^\circ$  and  $\theta_T = 0.6^\circ$ ). (d) The corresponding band structure has nonzero Chern numbers for the first two hole bands with the second hole band having a bandwidth  $\lesssim 10$  meV.

potential, we can rewrite our Hamiltonian as

$$\begin{aligned}
 H(k) = & \sum_G \epsilon(k+G) c_{k+G}^\dagger c_{k+G} \\
 & + \sum_{G, g^1} [M(k+G, k+G+g^1) c_{k+G}^\dagger c_{k+G+g^1} + \text{H.c.}] \\
 & + \sum_{G, g^2} [M(k+G, k+G+g^2) c_{k+G}^\dagger c_{k+G+g^2} + \text{H.c.}],
 \end{aligned} \tag{5}$$

where the creation and annihilation operators for Dirac spinors are written in the expansion basis for the specific  $k$  point. Shown in the schematic in Fig. 2(a) are  $G$  the complete set of super-moiré reciprocal lattice vectors (gray dots),  $g^1$  (blue dots), and  $g^2$  (red dots), which are the first stars of the reciprocal lattice vectors of the first and second moiré potentials, respectively. For a monolayer graphene active layer,  $\epsilon(k)$  is the Dirac Hamiltonian. For the moiré matrix elements  $M(\alpha, \beta)$ , we take the experimentally relevant parameter set from the analysis in Ref. [29].

This approach allows us to develop a conceptual understanding of how the flat band emerges. Without any super-moiré potential, we can still fold the bands into the mini-Brillouin zone. The lattice geometry gives rise to band

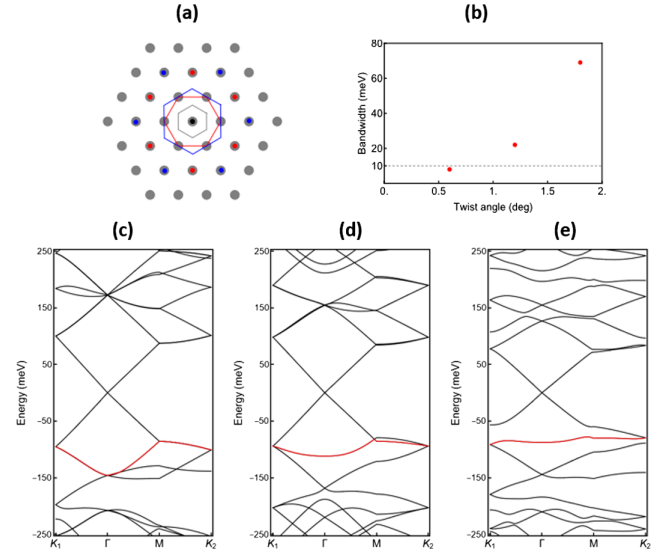


FIG. 2. Understanding the emergence of topological flat bands in monolayer graphene. (a) Schematic of the Brillouin zones and reciprocal lattice points of the super-moiré potential from the  $k$  point of interest represented by the black dot at the center. The red, blue, and gray lines (dots) show the first-, second-, and super-moiré Brillouin zones (shells), respectively. (b) Bandwidth of the second hole band increases as a function of twist angle  $\theta_T$  keeping  $\theta_B = 0^\circ$  fixed. (c) Band structure of the  $h$ -BN/G/ $h$ -BN heterostructure including only the top moiré potential, i.e., coupling only to the blue dots in (a). (d) Band structure of the  $h$ -BN/G/ $h$ -BN heterostructure including only the bottom moiré potential (red dots). (e) Band structure of the  $h$ -BN/G/ $h$ -BN with the super-moiré potential (gray dots). Similar to our results in Fig. 1, the symmetry-based approach also results in an isolated and flat second hole band. Not shown: If we use only a single moiré potential with the parameters in Ref. [29], we reproduce their results, finding one mini-Dirac point in the valance band and three mini-Dirac points in the conduction band.

touching at the points of high symmetry. We can then introduce the moiré potential as either a single-moiré potential [the second line in Eq. (5), represented by the red dots in Fig. 2(a)] or a super-moiré lattice potential [both the second and third lines in Eq. (5), represented by the gray dots]. The coupling of these terms to the plane wave states of graphene can open gaps at the high-symmetry points. Since the Dirac bands (comprised of the first electron and first hole band) acquire only a tiny gap at the  $\Gamma$  point [10], we focus instead on the second hole band. It was previously known (e.g., Refs. [9,29,31]) that, for the second hole band, a single-moiré potential opens a gap at the  $\Gamma$  point, while keeping the touching point at the  $K$  points (the so-called “secondary Dirac points”).

Zooming in close to the  $M$  point, we find that taking only the top moiré potential (blue dots) or just the bottom moiré potential (red dots) preserves the band touching [see Figs. 2(c) and 2(d)]. However, the super-moiré potential (gray dots) opens a gap that (perturbatively) is proportional to the product of the top and bottom moiré potentials. It is



this gap opening around the  $M$  point [see Fig. 2(e)] that makes the second hole band susceptible to isolation, while the longer real-space periodicity of the super-moiré potential acts to flatten this depinned band.

We, therefore, conclude that it is the coexistence of the last two lines in Eq. (5) that are responsible for the flat bands, making it an essential property of the super-moiré potential not present in either the single-moiré or aligned double-moiré potentials. This also explains the robustness of the observed phenomena with different models and parameter choices and suggests that it would also apply to other active layers beyond monolayer graphene (see below). While the opening of the gap at the  $M$  point can be understood from symmetry considerations, the flatness of the band depends quantitatively on the choice of parameters. For example, in Fig. 2(b), we show that for realistic parameters the bandwidth is increased for larger commensurate configurations. We have checked that, as expected by symmetry, the super-moiré lattice formed by the pair of twist angles ( $\theta^B = 0^\circ$  and  $\theta^T \approx 1.2^\circ$ ) opens gaps at the high-symmetry points. However, since the super-moiré potential is weaker, so are the avoided crossings, and we find that the bandwidth is about twice as large. We speculate that such a weak moiré potential with the right symmetry but insufficiently strong to generate an isolated flat band could explain the role of lattice relaxation seen in large-scale tight-binding numerical simulations [38].

*Hartree-Fock corrections.*—As discussed earlier, the modification to the band structure is due to the interference of moiré potentials, a purely single-particle effect. However, electrons in condensed matter systems interact with each other through the Coulomb potential, and this interaction becomes significant in flat-band systems. We study here the robustness of the flat band to Hartree-Fock shifts of the band structure. In what follows, we follow the formalism in Ref. [39], and we refer the reader there for technical details. Figure 3(a) shows the band structure of a monolayer with a super-moiré both with (red line) and without (dashed black line) the self-consistent Hartree potential. In sharp contrast to twisted bilayer graphene [39], the shape of the flat band is preserved after Hartree renormalization. In fact, the bandwidth is slightly diminished compared to the case without interactions. Since the second hole band remains flat and well separated from the rest of the bands, we expect that it will likely manifest experimental signatures of strongly correlated physics. The results presented in Fig. 3(a) illustrate the Hartree effect when filling the first hole band. We have verified that the robustness and isolation of the flat band persist even when the second hole band is filled, whether partially or completely. The observed changes remain minimal, with variations of less than 3 meV (refer to Supplemental Material [36]).

To further investigate the effect of the Hartree and Fock terms, we have calculated the density of states in three

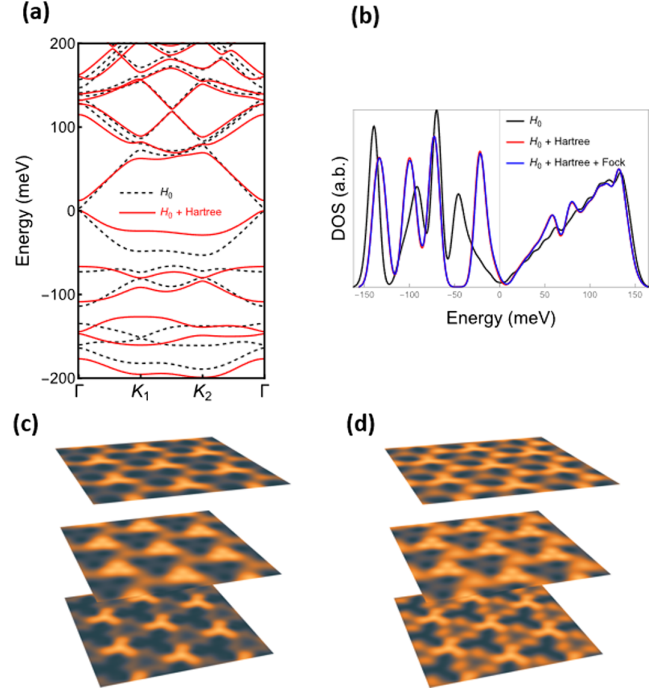


FIG. 3. Effect of Hartree-Fock potentials on electronic spectrum of super-moiré  $h$ -BN/G/ $h$ -BN heterostructure. (a) Non-interacting band structure without Hartree and Fock corrections (dashed black line) and band structure for the self-consistent Hartree charge distribution correction due to filling the first hole band (solid red line). (b) Density of states without Hartree-Fock corrections (black line), with only Hartree corrections (red line), and with both Hartree and Fock corrections (blue line). The addition of Fock potential does not alter the energy spectrum of the system. (c),(d) Charge distribution of the  $\Gamma$  point wave function without and with the effect of Hartree potential, respectively.

different scenarios. The results, which are illustrated in Fig. 3(b), show the density of states without interactions (black trace), with only the Hartree potential (red trace), and with both the Hartree and Fock potentials (blue trace). The blue and red traces are almost identical implying that the effect of the Fock potential is negligible in this system consistent with results on twisted bilayer graphene [39]. We also show how the electron-electron interaction redistributes the charge density in real space by plotting the modulus of the wave function of the  $\Gamma$  point both with and without the Hartree potential. We neglected spin and valley symmetry breaking in our implementation of the Hartree-Fock calculations. Studies that focus on such symmetry breaking (see, e.g., Ref. [40]), typically reveal very tiny (sub-meV) differences between the ground states. Moreover, these calculations are highly sensitive to atomic relaxation, external strain, and the details on the implementation of the Hartree calculation. In our view, this extreme sensitivity raises concerns about the reliability of the conclusions one can draw from such calculations.

*Generalization to bilayer and trilayer.*—Having discovered that a super-moiré potential significantly alters the electronic properties of monolayer graphene in unexpected ways, we test whether a super-moiré has similar effects on other graphene-based systems. We study the effect of super-moiré potentials on two other commonly used graphene systems: *AB* bilayer and *ABC* trilayer (Fig. 4). Remarkably, we find that the super-moiré potentials lead to the formation of topological flat bands in both bilayer graphene (where both the lowest-energy electron and hole bands have Chern numbers of  $\pm 1$ ) and in trilayer graphene. The trilayer case is even more interesting, since it supports larger Chern numbers. Flat bands with high Chern numbers are believed to support high-temperature superconductivity [41]. For bilayers and trilayers, the bands can be modified with an experimentally tunable displacement fields, and we show that with this additional degree of freedom, one can achieve very flat topological bands well separated from other bands.

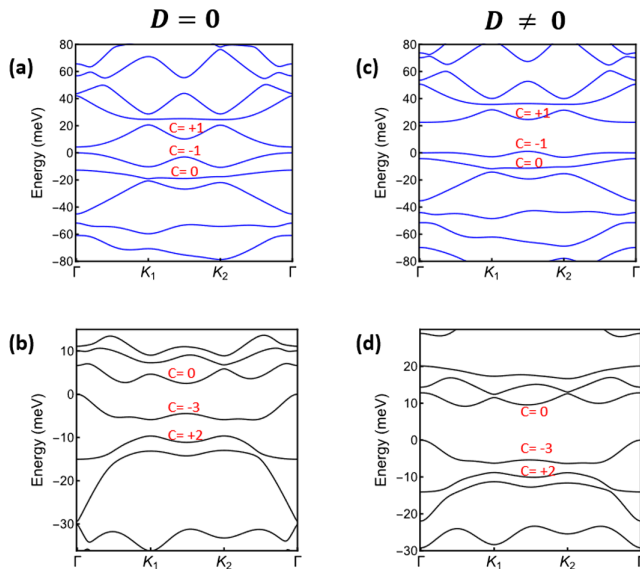


FIG. 4. Super-moiré topological flat bands in bilayer and trilayer graphene, with and without electric displacement field. (a) Low-energy bands of the *AB* bilayer graphene exposed to super-moiré potentials without external displacement field, displaying various flat bands around charge neutrality. The first electron and hole bands are topological with positive  $+1$  or negative  $-1$  Chern numbers, respectively. (b) Low-energy bands of the *ABC* trilayer graphene under super-moiré potential without an external displacement field, where the flat bands have Chern numbers greater than 1, which is different from the case of monolayer and bilayer. (c),(d) Energy bands of the *AB* bilayer and *ABC* trilayer graphene subjected to both super-moiré potential and external displacement field modeled by an electric potential energy difference of 40 meV. The indicated Chern numbers in (a) and (b) do not change in (c) and (d). The external displacement field adjusts the width of the low-energy bands, enhancing the diversity of possible experimental phase diagrams in the bilayer and trilayer graphene super-moiré systems.

*Conclusion.*—Our findings suggest that precise control of the alignment of the top and bottom *h*-BN substrates can result in a new platform for correlated physics. In this context, we note that recent advancements in controlling *h*-BN encapsulation of graphene with substantial yield [27] opens up this possibility. We, therefore, anticipate experimental results along these lines in the near future. We have demonstrated here that the interference of the two moiré potentials opens a gap in the mini Dirac points resulting in flat topological bands in untwisted 2D materials encapsulated by bulk misaligned substrates. We speculate that applying these ideas to twisted materials like twisted bilayer graphene, twisted double-bilayer, or twisted monolayer-bilayer graphene could result in further flattening of already flat bands or “superflat” bands. We leave these speculations for a future study.

It is a pleasure to thank Darryl Foo, Eugene Mele, and Giovanni Vignale for helpful discussions. We acknowledge the financial support of Singapore National Research Foundation Investigator Award (NRF-NRFI06-2020-0003) and the Ministry of Education AcRF Tier 2 Grant No. MOE-T2EP50220-0016. F.G. acknowledges support from the European Commission, within the Graphene Flagship, Core 3, Grant No. 881603 and from Grant No. SEV-2016-0686 and No. SprQuMat (Ministerio de Ciencia e Innovación, Spain) and NMAT2D (Comunidad de Madrid, Spain). J. H. and A. A. acknowledge the support by the Ministry of Education (MOE) Singapore under the Academic Research Fund Tier 2 (Grant No. MOE-T2EP50120-0015), MOE-AcRF Tier 1 (Grant No. A-8001967-00-00), and the National Research Foundation (NRF) of Singapore under its NRF-ISF joint program (Grant No. NRF2020-NRF-ISF004-3518).

- [1] A. H. Castro Neto, Francisco Guinea, Nuno M. R. Peres, Kostya S. Novoselov, and Andre K. Geim, The electronic properties of graphene, *Rev. Mod. Phys.* **81**, 109 (2009).
- [2] S. Das Sarma, Shaffique Adam, E. H. Hwang, and Enrico Rossi, Electronic transport in two-dimensional graphene, *Rev. Mod. Phys.* **83**, 407 (2011).
- [3] Valeri N. Kotov, Bruno Uchoa, Vitor M. Pereira, F. Guinea, and A. H. Castro Neto, Electron-electron interactions in graphene: Current status and perspectives, *Rev. Mod. Phys.* **84**, 1067 (2012).
- [4] Ho-Kin Tang, J. N. Leaw, J. N. B. Rodrigues, I. F. Herbut, Pinaki Sengupta, F. F. Assaad, and S. Adam, The role of electron-electron interactions in two-dimensional Dirac fermions, *Science* **361**, 570 (2018).
- [5] Da Zhan, Jiaxu Yan, Linfei Lai, Zhenhua Ni, Lei Liu, and Zexiang Shen, Engineering the electronic structure of graphene, *Adv. Mater.* **24**, 4055 (2012).
- [6] J. M. B. Lopes Dos Santos, N. M. R. Peres, and A. H. Castro Neto, Graphene bilayer with a twist: Electronic structure, *Phys. Rev. Lett.* **99**, 256802 (2007).

- [7] L. A. Ponomarenko, R. V. Gorbachev, G. L. Yu, D. C. Elias, R. Jalil, A. A. Patel, A. Mishchenko, A. S. Mayorov, C. R. Woods, J. R. Wallbank *et al.*, Cloning of Dirac fermions in graphene superlattices, *Nature (London)* **497**, 594 (2013).
- [8] Matthew Yankowitz, Qiong Ma, Pablo Jarillo-Herrero, and Brian J. LeRoy, van der Waals heterostructures combining graphene and hexagonal boron nitride, *Nat. Rev. Phys.* **1**, 112 (2019).
- [9] Matthew Yankowitz, Jeil Jung, Evan Laksono, Nicolas Leconte, Bheema L. Chittari, Kenji Watanabe, Takashi Taniguchi, Shaffique Adam, David Graf, and Cory R. Dean, Dynamic band-structure tuning of graphene moiré superlattices with pressure, *Nature (London)* **557**, 404 (2018).
- [10] Jeil Jung, Ashley M. DaSilva, Allan H. MacDonald, and Shaffique Adam, Origin of band gaps in graphene on hexagonal boron nitride, *Nat. Commun.* **6**, 6308 (2015).
- [11] Rafi Bistritzer and Allan H. MacDonald, Moiré bands in twisted double-layer graphene, *Proc. Natl. Acad. Sci. U.S.A.* **108**, 12233 (2011).
- [12] Ya-Hui Zhang, Dan Mao, Yuan Cao, Pablo Jarillo-Herrero, and T. Senthil, Nearly flat Chern bands in moiré superlattices, *Phys. Rev. B* **99**, 075127 (2019).
- [13] Yuan Cao, Valla Fatemi, Shiang Fang, Kenji Watanabe, Takashi Taniguchi, Efthimios Kaxiras, and Pablo Jarillo-Herrero, Unconventional superconductivity in magic-angle graphene superlattices, *Nature (London)* **556**, 43 (2018).
- [14] Yuan Cao, Valla Fatemi, Ahmet Demir, Shiang Fang, Spencer L. Tomarken, Jason Y Luo, Javier D. Sanchez-Yamagishi, Kenji Watanabe, Takashi Taniguchi, Efthimios Kaxiras *et al.*, Correlated insulator behaviour at half-filling in magic-angle graphene superlattices, *Nature (London)* **556**, 80 (2018).
- [15] Aaron L. Sharpe, Eli J. Fox, Arthur W. Barnard, Joe Finney, Kenji Watanabe, Takashi Taniguchi, M. A. Kastner, and David Goldhaber-Gordon, Emergent ferromagnetism near three-quarters filling in twisted bilayer graphene, *Science* **365**, 605 (2019).
- [16] Yonglong Xie, Andrew T. Pierce, Jeong Min Park, Daniel E. Parker, Eslam Khalaf, Patrick Ledwith, Yuan Cao, Seung Hwan Lee, Shaowen Chen, Patrick R. Forrester *et al.*, Fractional Chern insulators in magic-angle twisted bilayer graphene, *Nature (London)* **600**, 439 (2021).
- [17] Shuigang Xu, Mohammed M. Al Ezzi, Nilanthy Balakrishnan, Aitor Garcia-Ruiz, Bonnie Tsim, Ciaran Mullan, Julien Barrier, Na Xin, Benjamin A. Piot, Takashi Taniguchi *et al.*, Tunable van Hove singularities and correlated states in twisted monolayer–bilayer graphene, *Nat. Phys.* **17**, 619 (2021).
- [18] Shaowen Chen, Minhao He, Ya-Hui Zhang, Valerie Hsieh, Zaiyao Fei, Kenji Watanabe, Takashi Taniguchi, David H. Cobden, Xiaodong Xu, Cory R. Dean *et al.*, Electrically tunable correlated and topological states in twisted monolayer–bilayer graphene, *Nat. Phys.* **17**, 374 (2021).
- [19] Hryhoriy Polshyn, Jihang Zhu, Manish A. Kumar, Yuxuan Zhang, Fangyuan Yang, Charles L. Tschirhart, Marec Serlin, Kenji Watanabe, Takashi Taniguchi, Allan H. MacDonald *et al.*, Electrical switching of magnetic order in an orbital Chern insulator, *Nature (London)* **588**, 66 (2020).
- [20] Xiaomeng Liu, Zeyu Hao, Eslam Khalaf, Jong Yeon Lee, Yuval Ronen, Hyobin Yoo, Danial Haei Najafabadi, Kenji Watanabe, Takashi Taniguchi, Ashvin Vishwanath *et al.*, Tunable spin-polarized correlated states in twisted double bilayer graphene, *Nature (London)* **583**, 221 (2020).
- [21] Jeong Min Park, Yuan Cao, Li-Qiao Xia, Shuwen Sun, Kenji Watanabe, Takashi Taniguchi, and Pablo Jarillo-Herrero, Robust superconductivity in magic-angle multilayer graphene family, *Nat. Mater.* **21**, 877 (2022).
- [22] Zihao Wang, Yi Bo Wang, Jun Yin, Endre Tovari, Y Yang, L Lin, Matthew Holwill, John Birkbeck, D.J. Perello, Shuigang Xu *et al.*, Composite super-moiré lattices in double-aligned graphene heterostructures, *Sci. Adv.* **5**, eaay8897 (2019).
- [23] Lujun Wang, Simon Zihlmann, Ming-Hao Liu, Péter Makk, Kenji Watanabe, Takashi Taniguchi, Andreas Baumgartner, and Christian Schonenberger, New generation of moiré superlattices in doubly aligned *h*-BN/graphene/*h*-BN heterostructures, *Nano Lett.* **19**, 2371 (2019).
- [24] Nathan R. Finney, Matthew Yankowitz, Lithurshanaa Muraleetharan, K Watanabe, T Taniguchi, Cory R. Dean, and James Hone, Tunable crystal symmetry in graphene–boron nitride heterostructures with coexisting moiré superlattices, *Nat. Nanotechnol.* **14**, 1029 (2019).
- [25] Aviram Uri, Sergio C. de la Barrera, Mallika T. Randeria, Daniel Rodan-Legrain, Trithap Devakul, Philip J. D. Crowley, Nisarga Paul, Kenji Watanabe, Takashi Taniguchi, Ron Lifshitz *et al.*, Superconductivity and strong interactions in a tunable moiré quasiperiodic crystal, *Nature (London)* **620**, 762 (2023).
- [26] Xingdan Sun, Shihao Zhang, Zhiyong Liu, Honglei Zhu, Jinqiang Huang, Kai Yuan, Zhenhua Wang, Kenji Watanabe, Takashi Taniguchi, Xiaoxi Li *et al.*, Correlated states in doubly-aligned *h*-BN/graphene/*h*-BN heterostructures, *Nat. Commun.* **12**, 7196 (2021).
- [27] Junxiong Hu, Junyou Tan, Mohammed M. Al Ezzi, Udvat Chatteropadhyay, Jian Gou, Yuntian Zheng, Zihao Wang, Jiayu Chen, Reshmi Thottathil, Jiangbo Luo *et al.*, Controlled alignment of supermoiré lattice in double-aligned graphene heterostructures, *Nat. Commun.* **14**, 4142 (2023).
- [28] Jinhai Mao, Slavisa P. Milovanović, Misa Anđelković, Xinyuan Lai, Yang Cao, Kenji Watanabe, Takashi Taniguchi, Lucian Covaci, Francois M. Peeters, Andre K. Geim *et al.*, Evidence of flat bands and correlated states in buckled graphene superlattices, *Nature (London)* **584**, 215 (2020).
- [29] J. R. Wallbank, A. A. Patel, M Mucha-Kruczyński, A. K. Geim, and V.I. Fal’Ko, Generic miniband structure of graphene on a hexagonal substrate, *Phys. Rev. B* **87**, 245408 (2013).
- [30] Pablo San-Jose, A. Gutiérrez-Rubio, Mauricio Sturla, and Francisco Guinea, Spontaneous strains and gap in graphene on boron nitride, *Phys. Rev. B* **90**, 075428 (2014).
- [31] Jeil Jung, Evan Laksono, Ashley M. DaSilva, Allan H. MacDonald, Marcin Mucha-Kruczyński, and Shaffique Adam, Moiré band model and band gaps of graphene on hexagonal boron nitride, *Phys. Rev. B* **96**, 085442 (2017).
- [32] Pilkyung Moon and Mikito Koshino, Electronic properties of graphene/hexagonal-boron-nitride moiré superlattice, *Phys. Rev. B* **90**, 155406 (2014).

- [33] Christian Mouldale, Angelika Knothe, and Vladimir Fal'ko, Kagome network of miniband-edge states in double-aligned graphene–hexagonal boron nitride structures, *Phys. Rev. B* **105**, L201112 (2022).
- [34] R. M. Ribeiro and N. M. R. Peres, Stability of boron nitride bilayers: Ground-state energies, interlayer distances, and tight-binding description, *Phys. Rev. B* **83**, 235312 (2019).
- [35] H. Y. Lee *et al.*, Tunable Optical Properties of Thin Films Controlled by the Interface Twist Angle, *Nano Lett.* **21**, 2832 (2021).
- [36] See Supplemental Material at <http://link.aps.org/supplemental/10.1103/PhysRevLett.132.126401> for filling dependence of Hartree energy and the robustness of the flat band with respect to the number of hBN layers used to model the hBN substrates.
- [37] Klaus Hermann, Periodic overlayers and moiré patterns: Theoretical studies of geometric properties, *J. Phys. Condens. Matter* **24**, 314210 (2012).
- [38] Misa Andelkovic, Slavisa Milovanovic, Lucian Covaci, and Francois M. Peeters, Double moiré with a twist: Supermoiré in encapsulated graphene, *Nano Lett.* **20**, 979 (2020).
- [39] Tommaso Cea, Niels R. Walet, and Francisco Guinea, Electronic band structure and pinning of Fermi energy to van Hove singularities in twisted bilayer graphene: A self-consistent approach, *Phys. Rev. B* **100**, 205113 (2019).
- [40] Jihang Zhu, Iacopo Torre, Marco Polini, and Allan H. MacDonald, GW Theory of Magic-Angle Twisted Bilayer Graphene, [arXiv:2401.02872](https://arxiv.org/abs/2401.02872).
- [41] Sebastiano Peotta and Päivi Törmä, Superfluidity in topologically nontrivial flat bands, *Nat. Commun.* **6**, 8944 (2015).